This is a peer-reviewed, author's accepted manuscript of the following conference paper:
Chen, D., Marshall, B., Foote, C., Rangasamy, S., & Tian, S. (2023).
Towards HVDC interoperability - assessing existence of equilibrium with reference to converter terminal behaviour.
Paper presented at The 19th International Conference on AC and DC Power Transmission, Glasgow, United Kingdom.

Towards HVDC Interoperability - Assessing Existence of Equilibrium with Reference to Converter Terminal Behaviour

Dong Chen[1*], Benjamin Marshall[1], Colin Foote[1], Suresh Rangasamy[1], and Shangen Tian[1,2]

[1]The National HVDC Centre, SSEN Transmission, Cumbernauld, United Kingdom
[2]Department of Electronic and Electrical Engineering, University of Strathclyde, Glasgow
**dong.chen@sse.com*

Keywords: HVDC, INTEROPERABILITY, EQUILIBRIUM, IMPLICIT FUNCTION, VOLTAGE DROOP

Abstract

A key challenge to enable the interoperability of a Multi-Vendor-Multi-Terminal (MVMT) HVDC network is to assess the stability without requiring open sharing of the vendor Intellectual Property (IP) relating to control functions. An analytical criterion is therefore proposed as a first step of this assessment. The criterion is indexed by the margin against loss-of-equilibrium for a MVMT-HVDC network with terminal behaviour of connected converters. Based on a classical control architecture, a static analytical model is established, including relevant parameters within the DC network, its topology and operation. By linearizing the system at 0 Hz, the principle of assessing the singularity of the matrix of extended conductance is proposed and proved with the theorem of implicit function and principle of analytic continuation. Two types of scaler index are proposed and then normalized to indicate the margin against loss-of-equilibrium. The effectiveness of the indices is verified and analysed with simulations in the environments of both *Matlab/Simulink* and RTDS with pseudo-steady-state and detailed Electro-Magnetic Transient (EMT) modelling, respectively. This approach attempts to represent one MVMT control scheme to support practical specification, testing and demonstration of the first multi-vendor multi-terminal HVDC control system outside of China.

1 Introduction

Towards a net-zero electricity system, mass utilization of offshore wind energy has been identified as an enabler by the UK government [1] . Within the Holistic Network Design [2] for the GB system to 2030, a range of Multi-Terminal High Voltage Direct Current (MT-HVDC) transmission systems have been considered as an effective and economical approach to transmit bulk offshore power to the existing onshore power network [3]. These more extensive DC networks which are set to emerge are doing so coincident with an unprecedented growth of demand for HVDC worldwide and the need for Transmission System Operators (TSOs) to describe staged growth of and control paradigms for these DC networks. In this context, the need for MVMT HVDC solutions becomes increasingly likely.

Within GB, the Caithness Moray Shetland project (C-M-S) [4] is the first example of a multi-terminal VSC-HVDC system outside of China, although this has been delivered by a single vendor. In pilot projects elsewhere involving multiple vendors, it is understood that the vendors have been required to both open up areas of IP relating to control design and to modify their designs to make them compatible with other converters. This sort of open IP approach is not practical within GB and other international markets. There is a need for a practical approach to MVMT HVDC control without the requirement for vendors to divulge IP or for a third party to take responsibility for control design on every converter.

To address this gap need for a practical approach to MVMT HVDC control without the requirement to divulge and take responsibility for the IP and its adaptation of each vendor involved in such a system, The National HVDC centre and SSE Networks have proposed, and are taking forward a Pathfinder to 2030 project “Project Aquila” to demonstrate the first MVMT HVDC arrangement outside of China, utilising the principles of managing MVMT HVDC control to a strategy this paper seeks to define, and which is subject to a filed patent to protect its use for such purposes.

MVMT HVDC is a larger topic than control alone, bridging other areas such as process and interfacing alignment. These are not topics this paper will intrude upon but may be subject to future publications. The principal challenge of MVMT control interoperability is how to ensure HVDC converters of different vendor solutions can work together and maintain stability in a coupled DC network without sharing details of their internal designs, especially at the planning and procurement stage [5].

By introducing constant power terminals driven by the dynamics of offshore wind or onshore TSO dispatch, a MT-HVDC system is a non-linear system. Aligning with Lyapunov’s First method [6], stability assessment of a non-linear system includes two successive components, namely the existence of equilibrium and the sufficiency of damping. Although there has been lots of work about the stability of a DC system in both aspects, to the authors’ best knowledge,

there has not been a comprehensive solution that can ensure both aspects without detailing the internal control of the participating converters. Hence, there is a gap in supporting industrial application of MVMT HVDC.

In a multi-terminal DC network, a common principle is that at least one terminal must be under closed-loop voltage regulation [7]. This is to ensure power balancing and voltage regulation of the network can be maintained simultaneously. To improve the resilience of a MT-HVDC against loss of the slack DC terminal, control strategies of multiple voltage droops have been proposed to preserve voltage control in N-1 conditions and avoid control hunting between integral regulators [8]. Such an approach has a benefit in resilience provided the control priorities of such an approach can be defined effectively by the TSO in a manner that respects the characteristics of the converter response to the objective. To date the black-boxed nature of these components and lack of clarity in the control architecture required have limited the ability to achieve this. For example, the interactions of droop co-efficient will not only impact the operating point but also small-signal behaviour for which an acceptable control margin must be maintained. The range of voltage variation within the DC system and operating range may be co-ordinated and regulated by the multi-vendor control to a range of priorities for a range of operating points. A fair criterion to both assess and define the adequacy in the fore cited context is absent, and needs to be presented from a TSO perspective of compatible operation with the interfacing onshore AC transmission system.

As one step towards assessing control interactions in a MVMT-HVDC, a simple method is proposed in this paper to quantify the interactions between converters against loss-of-equilibrium. Without the information of internal design of converters, this method seeks to define the effect of converter response to a variation in terminal voltage such that conditions of stable operation may be identified and directed accordingly. This requires representation of the encrypted control detail within a model / replica in the form of an equivalent control droop response to the voltage change, for a given operating condition. Within that data provision, this method can quantify the compatibility of multiple droop coefficients considering the impact of operating point and network metrics. Aligning with the principle of Lyapunov's First method, this step will serve as a prerequisite and is decoupled from the assessment of small-signal stability before completing stability assessment for steady state.

The rest of the paper is organized as follows. The layout, control architecture, and associate component models of a typical offshore MT-HVDC are introduced in Section 2. It is followed by the principle of the proposed assessment in Section 3. After that, the effectiveness of the proposed methodology is verified in Section 4 by time domain simulations with a pseudo-steady state model and detailed EMT Multi-Modular Converter (MMC)-VSC model, using *Matlab*/*Simulink* and RTDS, respectively. Finally, the conclusion is drawn in Section 5.

2. Methodology

2.1 Benchmark System and Analytical Model

An illustrative multi-terminal HVDC network interconnecting offshore windfarms and an onshore AC transmission network is considered in this paper. The generic layout of the system is as in Fig. 1.

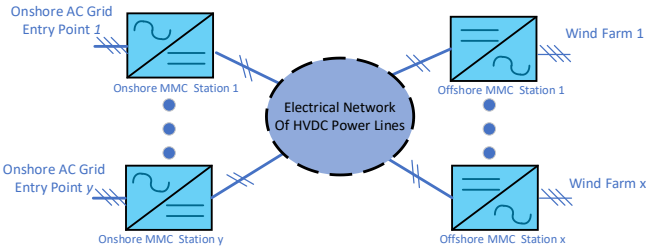

Fig. 1 Generic layout of offshore MTMV - HVDC

As shown in Fig. 1, the network consists of two types of HVDC terminal, namely an offshore interfacing Wind Farm (WF) terminal and Onshore (OS) terminal. In principle the more converters participate in the voltage control of the DC network, the greater the flexibility of this control will be; at least one terminal must provide this capability for the overall DC network to be controlled. However, the control of the DC network is subject to practical restrictions in respecting onshore and offshore AC system requirements.

For the offshore AC system providing offshore wind farm interface, it is normally necessary for grid forming control to be established where the HVDC converter defines the frequency and the voltage of the offshore island, thereby representing to the DC system a fixed power flow independent of DC dynamics in its steady state operation. This needs to be accounted for in the overall solution of the DC network but does not provide further flexibility in defining that solution but rather operates as a consequence of the DC voltage as defined elsewhere within this system, within the range of DC voltage available. Onshore the connection interfaces may be operated to a specific intended power flow which does not preclude being set based on a droop power control of the voltage within the DC network, but equally would be dependent also on the operating state of the onshore AC system at the time. Direct control of the AC system, for example at the point of offtake, can be introduced but in the example above would then limit the MVMT network to one point of voltage control and an associated vulnerability to its loss.

2.2 Architecture of System Control

Based on the scenarios in Section 2.1, a generic control architecture is assumed as Fig. 2 shows. As shown, each converter station is equipped with inner loops of current control, or equivalent. Among them, the characteristics of lower-level design, are aggregated and masked for the protection of vendors' Intellectual Property (IP). The masked designs include (voltage) regulators of current loops, AC voltage controls, modulation scheme, voltage balancing among sub-modules/arms/phases, main circuit, and other controls related to topology and the converter operating

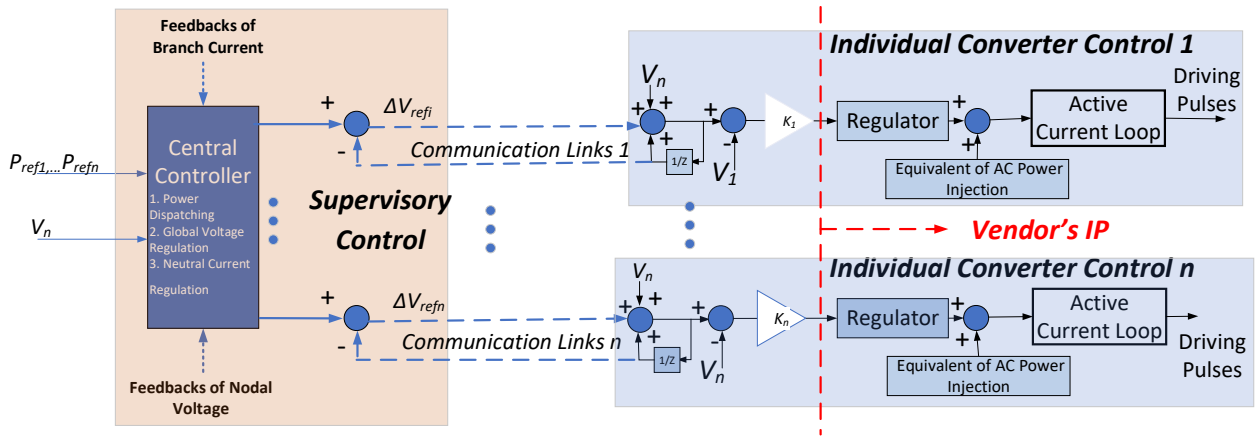

Fig. 2. Control Architecture of MTMV – HVDC

principles in respect to both the AC and DC systems. It is expected that at given extreme conditions of either the DC network or the associated converter operation the expression of control may be exposed to non-linearity and the objective of the supervisory control is to ensure that these are not conditions that either the network nor individual converters are exposed to in steady state or post-steady-state operation; the later representing a range of N-1 and other contingencies informing control priority and associated control margin.

The functions of supervisory control are implemented by a central control unit, which would be owned by the TSO. Based on the feedback measurements of voltages and currents along with input orders of power dispatching and nominal voltage, the outputs of the supervisory control will update the incremental values of DC voltage reference to converters via communication links. As the name implies, the intention of the supervisory control is to course-correct the operation of the overall system towards a steady state condition both stable and contingency robust. In this manner the concept is not dependent on the reliability of communication links as operation for a given condition would remain stable for that operating condition and a range of credible situations ahead of any further update. Actions via the supervisory control would act to slowly modify voltage reference responses by the associated converter terminals to correct and drive more secure new operating conditions for the DC network, and transitions of operating state can be implemented via a forward guidance of slow changes over an extended period of time, for example achieving a ramping up or down of power flow.

2.3 Nodal Model of DC Network

For assessment of interoperability, an MTMV-HVDC system is modelled as an electrical circuit with shunt controllable sources at selected nodes. The nodes represent the positions of converter terminals and junctions of cables within the DC network.

Each branch of the circuit characterizes the aggregated impedance of a corresponding point-to-point DC cable between two nodes and the connected series elements, such as DC circuit breaker, DC reactor, etc. if applicable.

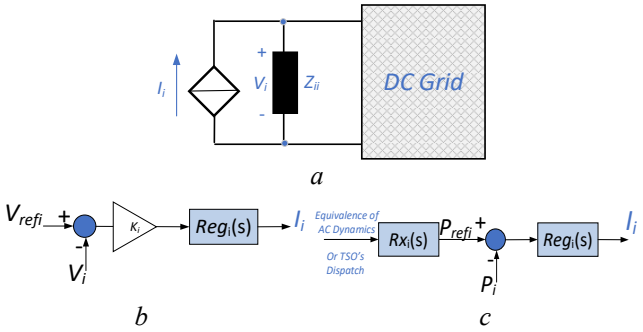

Fig. 3. HVDC Component Model (a) Nodal Equivalent, (b) Voltage-dependent Control, (c)Voltage-independent Control

Each node is modelled as a Norton Equivalent, as Fig. 3 (a) shows. The current source of the nodal equivalent is controllable and represents the active control of converter. The shunt impedance represents the shunt passive elements at the node, e.g. the aggregated capacitances of MMC cells and inductances, dump resistor, etc. DC junctions are modelled as special nodes where the order of the controllable current source is zero.

During operation, the nodes of converter terminals are categorized into two types, namely voltage-dependent and voltage-independent.

The model of voltage-dependent control is demonstrated in Fig. 3(b). Assuming the modulation process of the HVDC converter is linearized, the S-domain admittance of converter control is modelled as the product of K_i and $Reg_i(s)$ such that

$$\begin{cases} K_i = \left.\dfrac{I_i(s)}{V_{refi}(s)-V_i(s)}\right|_{s=0} \\ Reg_i(s) = \dfrac{I_i(s)}{K_i[V_{refi}(s)-V_i(s)]} \end{cases} \quad (1)$$

where I_i, V_{refi}, and V_i represent the reference voltage order, terminal voltage, and output current of active control at node i. Therefore, when it is under voltage dependent control, the order of the controllable current source of a voltage-dependent node can be expressed as

$$I_i(s)|_{s=0} = K_i(V_{refi} - V_i) \quad (2)$$

For a node with voltage-independent control, the control of constant power is mainly considered in this paper (as constant DC current control is rare and does not change nodal shunt impedance at 0 Hz). The equivalent power order is assumed to be a result of either a local converter control mechanism, e.g. autonomously balancing the connected AC network [9] or the dispatch order of operator. In both cases, the output power is determined by a one-way input to the DC system. Projecting to the control mechanism shown in Fig. 3(c), at steady state, there is

$$\begin{cases} Rx_i(s)|_{s=0} = 1 \\ Reg_i(s)|_{s=0} = 1 \\ I_i(s)|_{s=0} = P_{refi}(s)/V_i(s)|_{s=0} \end{cases} \quad (3)$$

2.4 Branch Model of DC Network

For each DC branch, including both the positive and negative poles to give a return path, between Node i and j, the aggregated impedance $Z_{ij}(s)$ at steady state is written as

$$Z_{ij}(s)|_{s=0} = R_{ij} \quad (4)$$

where $R_{ij}(i \neq j)$ is the aggregated resistance of the branch, including return; R_{ii} is the shunt resistance at the ith node.

3 Principle of Assessing Existence of Equilibrium

3.1 Network Model at Steady State

By interconnecting n nodal equivalents shown in Fig. 3(a) with a branch return in between any two nodes, the equilibriums of an n-node HVDC network can be characterized with Kirchhoff's law [10] for voltage as

$$\boldsymbol{G}\vec{V} = \vec{I} \quad (5)$$

where $\boldsymbol{G}$ is an $n \times n$ symmetrical matrix of network conductance; $\vec{V}$ the n–dimension vector of nodal voltage; $\vec{I}$ the n –dimension vector of nodal current injection from converters. Representing the element of $\boldsymbol{G}$ at ith ($0<i\leqslant n$) row and jth ($0<j\leqslant n$) column with G_{ij} gives

$$\begin{cases} G_{ji} = G_{ij} = -\frac{1}{R_{ij}} \\ G_{ii} = \sum_{i=1}^{n} \frac{1}{R_{ij}} \end{cases} \quad (6)$$

The ith component of $\vec{V}$ is V_i and ith component of $\vec{I}$ is I_i. Considering the control in Fig. 2 and Fig. 3, the vector of nodal current injection can also be expressed as

$$\vec{I} = \boldsymbol{K}\left(\overrightarrow{V_{ref}} - \vec{V}\right) + \boldsymbol{INV}\overrightarrow{P_{ref}} \quad (7)$$

where $\boldsymbol{K}$ is an $n \times n$ diagonal matrix of droop gain. Its diagonal element at ith row K_i ($0 < i \leq n$) represents the voltage droop coefficient of the ith node; if the node is not droop controlled, then $K_{ii} = 0$. $\overrightarrow{V_{ref}}$ is an n-dimension vector of the reference value of droop control, whose ith ($0<i\leq n$) component is V_{refi}; $\boldsymbol{INV}$ is an $n\times n$ diagonal matrix, whose diagonal element $\boldsymbol{INV_i}$ ($0<i\leqslant n$) is $\frac{1}{V_i}$; $\overrightarrow{P_{ref}}$ is an n-dimension vector of the arbitrary power injection at all the nodes, whose ith ($0<i\leqslant n$) component P_{refi} represents the expected power injection at the ith node.

Substituting (7) into (5), one can define a function

$$\boldsymbol{F}\left(\vec{V}, \overrightarrow{P_{ref}}\right) = (\boldsymbol{G}+\boldsymbol{K})\vec{V} - \boldsymbol{K}\overrightarrow{V_{ref}} - \boldsymbol{INV}\overrightarrow{P_{ref}} = \boldsymbol{0} \quad (8)$$

Let the vector $\vec{V}$ be a dependent variable driven by the independent variable $\overrightarrow{P_{ref}}$, then the corresponding function of solution to $\vec{V}$, $\vec{V} = f(\overrightarrow{P_{ref}})$, is implicitly defined by the function of $\boldsymbol{F}\left(\vec{V}, \overrightarrow{P_{ref}}\right)$.

If a converter node is designed to operate either as voltage-independent or voltage-dependent exclusive, then this assumption can be mathematically expressed as

$$K_i P_{refi} = 0 \quad (9)$$

3.2 Assessing existence of equilibrium

Based on the definition in (9), for a practical design of HVDC network, the function of $\boldsymbol{F}\left(\vec{V}, \overrightarrow{P_{ref}}\right)$ is a linear combination of polynomial functions and reciprocal functions; hence it is continuously differentiable and analytic [11] with respect of all elements of $\vec{V}$ and $\overrightarrow{P_{ref}}$. By applying the theorem of implicit function [12] to (9), there must be a unique function of $f(\overrightarrow{P_{ref}})$ in the neighbourhood of (or an open set that contains) an operating point ($\overrightarrow{V_0}, \overrightarrow{P_{ref0}}$), as long as the following two conditions both stand:

Condition (I): One equilibrium does exist at the operating point of ($\overrightarrow{V_0}, \overrightarrow{P_{ref0}}$).

Condition (II): The Jacobian matrix of $\boldsymbol{F}\left(\vec{V}, \overrightarrow{P_{ref}}\right)$ with respect of $\vec{V}$ is not singular at the equilibrium. That is

$$\left|\frac{\partial \boldsymbol{F}(\vec{V}, \overrightarrow{P_{ref}})}{\partial V_1, \partial V_2, \cdots, \partial V_n}\right|\Bigg|_{\vec{V}=\overrightarrow{V_0}, \overrightarrow{P_{ref}}=\overrightarrow{P_{ref0}}} \neq 0 \quad (10)$$

By complying with Condition (II), the domain of the fore cited implicit function $f(\overrightarrow{P_{ref}})$ is expandable by iteratively repeating the following steps: 1) selecting one new equilibrium of on the boundary of the neighbourhood to satisfy Condition (I); 2) then satisfying Condition (II) based on the new equilibrium again.

By iteratively expanding the domain, the operating point can be expanded throughout a set of manifolds that consistently complies with (8) and Condition (II); hence the existence of equilibrium is ensured throughout this aggregated manifold. This process is aligned with the principle of analytic continuation [11]. Substituting (8) into (10) yields

$$|\boldsymbol{G} + \boldsymbol{K} - \boldsymbol{INVS}| \neq 0 \quad (11)$$

where $\boldsymbol{INVS}$ is an $n \times n$ diagonal matrix, whose diagonal element on ith row, $INVS_{ii}$ $(0 < i \leq n)$ is $\frac{-P_{refi}}{V_{i0}^2}$. Define $\boldsymbol{G_{ex}}$ as the extended conductance matrix with

$$\boldsymbol{G_{ex}} = \boldsymbol{G} + \boldsymbol{K} - \boldsymbol{INVS} \tag{12}$$

For a practical HVDC network, the operating points of power must be bounded. To ensure the condition of (10) consistently stands within a bounded space of power vector defined by

$$\boldsymbol{P} = \left\{P_{ref1,}P_{ref2,\cdots,}P_{refn} \middle| P_{mini} \leq P_{refi} \leq P_{maxi}\right\} \tag{13}$$

any one of the following two conditions shall exclusively stand for all eligible operating points $(\overrightarrow{V_0}, \overrightarrow{P_{ref0}})$ that satisfies the condition of $\overrightarrow{P_{ref0}} \in \boldsymbol{P}$:

Condition 1:

$$|G_{ex}| > 0 \tag{14}$$

Condition 2:

$$|G_{ex}| < 0 \tag{15}$$

And therefore, the operational margin against loss-of-equilibrium can be defined as $|G_{ex}|$, whose greater value indicate a better margin.

Considering the extended conductance matrix is real and symmetrical by its mathematical definition, **Condition 1** (14) can be replaced by a sufficient (enhanced) condition that the extended conductance matrix is positive definite as it will guarantee its leading principal minor of all orders, which include its determinant, are all positive [13],[14], which is expressed as

Condition 3:

$$G_{ex} > 0 \tag{16}$$

or equivalently ensure a minimum eigen value of G_{ex} is positive [13, 14]

$$\lambda_{min}(G_{ex}) > 0 \tag{17}$$

Similarly, **Condition 2** (15) can be replaced by an enhanced condition of consistent negative definiteness of the extended conductance G_{ex} throughout the space of $\boldsymbol{P}$ as

Condition 4:

$$G_{ex} < 0 \tag{18}$$

or equivalently the negativity of greatest eigen value as

$$\lambda_{max}(G_{ex}) < 0 \tag{19}$$

For the enhanced conditions, the operational margin against loss-of-equilibrium can be expressed by $\lambda_{max}(G_{ex})$ or $\lambda_{min}(G_{ex})$ when the extended conductance matrix, G_{ex}, is positive definite or negative definite, respectively.

3.3 Initial equilibrium and refined assessment criteria

The existence of equilibrium in an HVDC system can be guaranteed in every cycle of control by iteratively complying with Conditions (I) and (II) and securing a pre-defined margin with (14), (15), (17), (19). As a start of the iteration, an initial equilibrium of operating point must be guaranteed for Condition (I).

Naturally, this initial equilibrium can be practically selected as the condition of a no-load condition. Mathematically, such condition is represented by assigning 0 to all the components of $\overrightarrow{P_{ref}}$ in (8).

Therefore, the initial operating point to the operating voltage vector $\vec{V} = \overrightarrow{V_{ini}}$ is always solvable from (8) as

$$\overrightarrow{V_{ini}} = -(\boldsymbol{G} + \boldsymbol{K})^{-1}\boldsymbol{K}\overrightarrow{V_{ref}} \tag{20}$$

as long as the following condition stands [14]

$$|\boldsymbol{G} + \boldsymbol{K}| \neq \boldsymbol{0} \tag{21}$$

In an HVDC system, the probability of not satisfying (21) is practically zero. By assigning the nominal value of DC voltage V_n (>0) to every component of the voltage reference vector $\overrightarrow{V_{ref}}$, every component of initial voltage $\overrightarrow{V_{ini}}$ shall stay at the nominal value and therefore the initial equilibrium is secured to satisfy Condition (I). At this initial condition, there is

$$\boldsymbol{G_{ex}}|_{\overrightarrow{P_{ref0}}=\boldsymbol{O_{1\times n}}} = \boldsymbol{G_{exini}} = \boldsymbol{G} + \boldsymbol{K} = \boldsymbol{G_s} + \boldsymbol{G_m} + \boldsymbol{K} \tag{22}$$

where $\boldsymbol{G_s}$ is defined as a diagonal matrix of self-conductance of the HVDC network and its diagonal elements G_{sii} will be defined as the reciprocal of shunt (self) resistance

$$G_{sii} = \frac{1}{R_{ii}} \qquad G_{sii} \in [0, +\infty) \tag{23}$$

Substituting (6) and (23) into (21), one can obtain the elements of the mutual conductance matrix $\boldsymbol{G_m}$ as

$$\begin{cases} G_{mji} = G_{mij} = -\frac{1}{R_{ij}} & (i \neq j) \\ G_{mii} = \sum_{i=1}^{n} \frac{1}{R_{ij}} & (i \neq j) \end{cases} \tag{24}$$

Considering the mutual conductance matrix $\boldsymbol{G_m}$ is a Laplace matrix by its definition in (24) and the positivity of all branch resistance, i.e. $R_{ij} \in (0, +\infty]$, $\boldsymbol{G_m}$ must be semi-positive definite [15]. Thus, for any non-zero n-dimension real vector $\vec{X}$, the quadratic form of $\boldsymbol{G_m}$ shall comply with [13, 14]

$$\vec{X}\boldsymbol{G_m}\vec{X}^T \geq 0 \tag{25}$$

As a practical design of droop coefficient must be greater or equal to zero, the diagonal elements of the diagonal matrix $\boldsymbol{K}$ must be greater or equal to zero; considering (22), so must $\boldsymbol{G_s}$. Therefore, there is

$$\begin{cases} \vec{X}\boldsymbol{G_S}\vec{X}^T \geq 0 \\ \vec{X}\boldsymbol{K}\vec{X}^T \geq 0 \end{cases} \quad (26)$$

Summing up the inequations of (25)(26) on both sides of the operators, one can write the following to prove the semi-positive definiteness of the extended conductance matrix $\boldsymbol{G_{ex}}$ at the initial energization condition as

$$\vec{X}(\boldsymbol{G_m}+\boldsymbol{G_m}+\boldsymbol{K})\vec{X}^T = \vec{X}\boldsymbol{G_{exini}}\vec{X}^T \geq 0 \quad (27)$$

Since the initial condition must be practically included in the expected manifold set of operating power, $\boldsymbol{P}$, Conditions 2 and 4 (in Section II-B) are therefore ruled out from practical scenarios of HVDC operation, as a semi-positive definite matrix $\boldsymbol{G_{exini}}$ can neither have a negative determinant nor eigen value [13],[14]. As a result, the assessment criteria to existence of equilibrium can be reduced to **Condition 1 or 3**.

3.4 Normalization of Assessment Margin

Although **Condition 1 or 3** can serve as a margin against loss-of-equilibrium, the actual implication of the value may vary significantly with variable structures of circuit or control. One consequence is that it is difficult for an operator to interpret the electrical implication of the resultant margin. This makes it difficult to set up a generic standard in specifying the requirement of an interoperable HVDC system for TSOs. Considering this, two types of normalized index, namely CX-index-I (corresponding to Condition 1) and CX-index-II (corresponding to Condition 3), are created to generically index an HVDC network of any topology and control structure as below:

CX-Index I:

$$Ind_{CX1} = \frac{|G_{ex}|}{|G_{exo}|} \quad (28)$$

CX-Index II:

$$Ind_{CX2} = \frac{\lambda(G_{ex})_{min}}{\lambda(G_{exo})_{min}} \quad (29)$$

Either index in (28) or (29) can adequately indicate the operating condition against loss-of-equilibrium. With both base values corresponding to no-load condition (zero transfer power) of the HVDC grid, when the value is closer to 1, it indicates a closer operating condition to a risk-free no-load status, whereas a value more towards 0 indicates higher risk of loss-of-equilibrium (voltage collapse).

To obtain the index of (28) or (29), the inputs are droop coefficients $\boldsymbol{K}$, network metrics $\boldsymbol{G}$, (expected or measured) power injections $\overrightarrow{P_{ref}}$, and measurements of terminal voltage $\vec{V}$. As required for interoperability, the information of internal design of converters are not required.

3.5 Inclusion of Supervisory Control

The extended matrix of conductance $\boldsymbol{G_{ex}}$ can be further expanded by including another component matrix of supervisory droop control, K_s as

$$\boldsymbol{G_{ex}} = \boldsymbol{G} + \boldsymbol{K} + \boldsymbol{K_S} - \boldsymbol{INVS} \quad (30)$$

where of K_s is an $n \times n$ matrix. Each of its elements K_{Sij} defines the weight of the voltage at jth node ($0<j\leqslant n$) towards a global reference value in regulating the voltage at ith node ($0<i\leqslant n$). This component is dispatched by a supervisory control function based on communications between converters and a central control unit. The impact of the communications will be reflected by its non-diagonal elements. Since the inclusion of supervisory control does not change the nature of the methodology, $\boldsymbol{K_S}$ is assumed to be a zero matrix for simplicity in the rest of the paper.

4 Case Studies

To verify the proposed methodology, a benchmark system is set up for case studies as Fig. 4 and Table 1 shows.

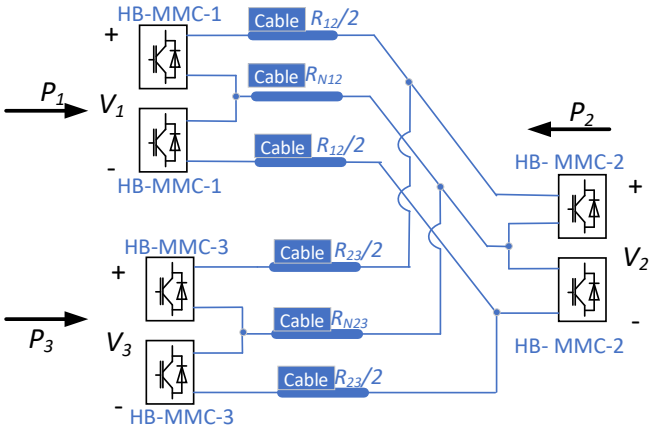

Fig. 4. Layout of 3-Terminal Benchmark

Table 1 Initial Parameter of 3-Terminal Benchmark

Parameter	Value
R_{12}, R_{12}	10 Ω, 10 Ω
Rated voltage	1050 kV (bipolar)
Valve Capacitance	29 μF (per pole)
K_1, K_3(equivalent to bipolar)	8.258 A/kV,8.258 A/kV
R_{n12}, R_{n12}	10 Ω, 10 Ω
Timesteps of Pseudo-steady-state, EMT simulation	100 μs (Tustin/Backward Euler), 3.57 μs (Dommel)
MMC Conduction Resistance for EMT Simulation (per arm)	0.56 Ω

As shown in Fig. 4, a 3-terminal bipolar HVDC network is illustrated with all the Half-Bridge Multi-Modular-Converters (HB-MMC) having identical current loops with bandwidth at 600 Hz (referring to an infinite AC bus connection) per pole and control frequency at 20 kHz. Lead-lag regulators are used for all DC regulators with lead and lag time constants at 0.004 s and 0.02 s, respectively. Terminal 2 is assigned as a constant power terminal with proportional gain of power

regulator at 0.1 kV/MW and time constant at 0.001 s, corresponding to the control scheme in Figure 2.

Two types of models are used for time-domain simulations, namely pseudo-steady state DC power flow and EMT. The pseudo-steady state simulation is carried out with *Matlab*/*Simulink* and the EMT with Real-Time-Digital-Simulation (RTDS). For pseudo-steady state simulation, all control and circuits are forced to steady state, i.e. $s = 0$ in the transfer functions; whereas in EMT models, generic average HB-MMC models are used with inter-arm and inter-phase balancing control included [16]. Besides, frequency dependent models of DC cables [17] are used to simulate DC cables in EMT simulations.

4.1 Verification of CX-Indices in DC Power Flow

To verify the proposed index, power ramp tests are carried out based on the benchmark system in Fig. 4 and Table 1. The results are shown in Fig. 5.

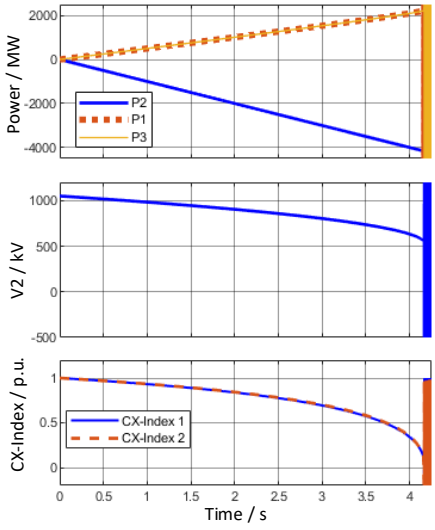

a

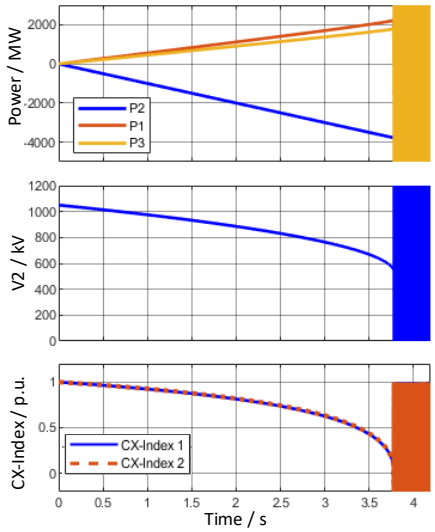

b

Fig. 5 Ramp Test with Pseudo-Steady-State Simulation (a) With initial droop coefficients (b) With Reduced Droop Coefficient

As shown in Fig. 5 (a), the system starts with the constant power terminal (Terminal 2) operating at 0 MW at Time = 0 s. When a power ramp of -1000 MW/s is applied to P_2, the other two terminals start to accommodate this power demand at the same scale as the droop coefficients and network metrics are symmetrical. As the constant power load grows, the voltage at Terminal 2, V_2, decreases from nominal value, 1050 kV. Meanwhile both CX indexes, *Ind-CX 1* and *Ind-CX 2* drops from 1, corresponding to no-load condition, towards 0, where the voltage collapse occurs at approx. 4.17 s. Once any of the CW-indexes reaches 0, all quantities start to oscillate chaotically.

As a comparison, the ramp test is repeated with droop coefficient of Terminal 3, K_3 reduced by 10% in Fig. 5(b). This is reflected by a lower power sharing of Terminal 3 in accommodating the constant power demand of Terminal 2. As a lower droop coefficient leads to a lower grid strength to accommodate the constant power load, the boundary of DC power transfer is reduced to about 3750 MW and collapses at 3.75 s, where both CW-indexes again reach zero. This collapse is earlier than in the previous case as expected.

4.2 Comparison between Pseudo-Steady State and EMT Simulations

To verify the effectiveness of the CX-index in an EMT simulation, which is closer to real-world performance, a comparison is made based on the case study carried out in Fig. 5(b). The results are shown in Fig. 6. As shown, identical power ramp is enforced at Time = 0.6 s. It can be seen that the EMT measurements of voltage at Terminal 2, V_2 and CX Index 1, are almost identical to the power flow results with errors of less than 0.2%. Considering the ramp of -1000 MW/s is much more adverse than reality and there are still converter losses not counted in DC pseudo-steady state simulations, the accuracy of the CX-index can be regarded as satisfactory.

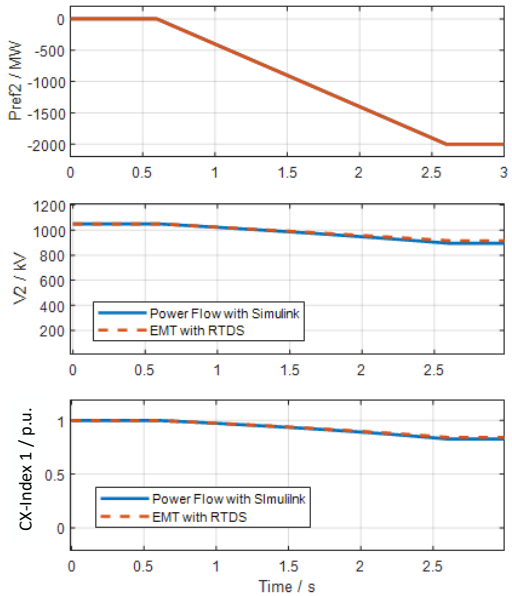

Fig. 6 Comparison between Pseudo-Steady-State and EMT

5 Conclusion

This paper provides a compact mathematical and simulation proof of the concept of a MVMT HVDC control paradigm not reliant upon the open disclosure, modification or standardization of the core Intellectual Property of a converter control. Rather via clear definition and solution of the DC network condition based upon the representation of the effect of the converter control, and a definition of margin in that operation relevant to steady state stability, an overall, non-vendor specific solution may be obtained in alignment to the TSO priorities for intended operation of the DC network. This therefore allows both the MVMT HVDC control and the associated converter contributions to it to be described, designed, specified, tested, and deployed with clear definition of individual vendor role and performance.

With reference to the proof, the proposed indices, namely CX-Index I and CX-Index II, can effectively quantify the interactions among converter droop co-efficient, the DC network metrics and operating points within a HVDC network. Either index can indicate the stability margin against DC power transfer limit, or equivalently loss-of-equilibrium, with a scaler between 0 and a positive value close to 1.

Although this indexing methodology is derived from static behaviour of an HVDC system, real time EMT simulations show that it can provide good accuracy in an online assessment from one steady state to a new steady state operation across a transition of a significant power ramp.

6 Acknowledgements

The authors would like to thank Prof. Huanhai Xin (Zhejiang University, China) for his advice on the use of mathematical theorems.

7 References

[1] HM Government Department for Business, Energy & Industrial Strategy. "Net Zero Strategy: Build Back Greener.". https://www.gov.uk/government/publications/net-zero-strategy (accessed 07 November, 2022).

[2] National Grid ESO. "The Pathway to 2030 Holisitic Network Design." https://www.nationalgrideso.com/future-energy/the-pathway-2030-holistic-network-design (accessed 07 November, 2022).

[3] Weixing Lu and Boon-Teck Ooi, "Premium quality power park based on multi-terminal HVDC," *IEEE Transactions on Power Delivery*, vol. 20, no. 2, pp. 978-983, April 2005.

[4] The National HVDC Centre. "Caithness-Moray HVDC Project During Delivery." https://www.hvdccentre.com/our-projects/caithness-moray/ (accessed 07 November, 2022).

[5] A. Shetgaonkar, L. Liu, A. Lekić, M. Popov, and P. Palensky, "Model predictive control and protection of MMC-based MTDC power systems," *International Journal of Electrical Power & Energy Systems,* vol. 146, p. 108710, 2023.

[6] M. S. M. Saat, S. K. Nguang, and A. Nasiri, *Analysis and synthesis of polynomial discrete-time systems: an SOS approach*. Butterworth-Heinemann, 2017.

[7] J. Beerten, D. Van Hertem, and R. Belmans, "VSC MTDC systems with a distributed DC voltage control-A power flow approach," in *2011 IEEE Trondheim PowerTech*, 2011: IEEE, pp. 1-6.

[8] J. Liang, T. Jing, O. Gomis-Bellmunt, J. Ekanayake and N. Jenkins, "Operation and Control of Multiterminal HVDC Transmission for Offshore Wind Farms," *IEEE Transactions on Power Delivery*, vol. 26, no. 4, pp. 2596-2604, Oct. 2011.

[9] D. B. Rathnayake *et al.*, "Grid forming inverter modeling, control, and applications," *IEEE Access,* 2021.

[10] R. L. Boylestad, *Introductory circuit analysis*. Pearson Education, 2013.

[11] R. Churchill and J. Brown, *Complex Variables and Applications*. McGraw Hill, 2014.

[12] S. G. Krantz and H. R. Parks, *The implicit function theorem: history, theory, and applications*. Springer Science & Business Media, 2002.

[13] A. J. Duran, "On orthogonal polynomials with respect to a positive definite matrix of measures," *Canadian Journal of Mathematics,* vol. 47, no. 1, pp. 88-112, 1995.

[14] G. Strang, G. Strang, G. Strang, and G. Strang, *Introduction to linear algebra*. Wellesley-Cambridge Press Wellesley, MA, 1993.

[15] E. Teufl and S. Wagner, "Determinant identities for Laplace matrices," *Linear algebra and its applications,* vol. 432, no. 1, pp. 441-457, 2010.

[16] D. Guo *et al.*, "Detailed quantitative comparison of half-bridge modular multilevel converter modelling methods," *The Journal of Engineering,* vol. 2019, no. 16, pp. 1292-1298, 2019.

[17] J. Beerten, S. D'Arco, and J. A. Suul, "Frequency-dependent cable modelling for small-signal stability analysis of VSC-HVDC systems," *IET Generation, Transmission & Distribution,* vol. 10, no. 6, pp. 1370-1381, 2016.